Radiophysics and Quantum Electronics, Vol. 43, No. 11, 2000

THE STRUCTURE OF A CHIRP SIGNAL IN THE RANDOMLY INHOMOGENEOUS EARTH–IONOSPHERE CHANNEL

N. T. Afanas'yev,[1] **V. P. Grozov,**[2] **V. E. Nosov,**[2] **and M. V. Tinin**[1]

UDC 621.371; 550.388.2

We analyze theoretically the structure of a chirp-ionosonde signal for the cases of one- and two-hop propagation in the randomly inhomogeneous ionosphere. For the case of two-hop propagation, wave scattering by the rough ground is taken into account. Our numerical simulation showed that random ionospheric irregularities and ground roughnesses play a significant role in the formation of a signal structure. We compare numerical results with experimental data obtained at oblique ionospheric sounding.

1. INTRODUCTION

At present, chirp ionosondes having good noise immunity, small power consumption, and high resolution are used for the ionospheric studies [1–6].

Although chirp ionosondes are widespread, the structure of chirp signals propagating in the ionospheric channel with allowance for the parameters of recording devices has not yet been studied in sufficient detail. Basically, the signal structure was analyzed in the absence of dispersion in the ionosphere or with allowance only for the phase dispersion in the case of propagation in a regular medium. This is explained by the absence of a detailed analysis of the chirp-signal structure in randomly inhomogeneous media taking background refraction into account [7–11].

It is well known that in the case of oblique ionospheric sounding, the signal at the reception point is formed, first of all, due to wave propagation in the ionosphere without intermediate reflections from the ground. On the other hand, the signal can propagate by means of subsequent reflections from the walls of the Earth–ionosphere waveguide. Below we will consider these two possibilities of the formation of a continuous chirp signal. However, in the second case, for simplicity, we restrict ourselves to the analysis of signal behavior for two-hop propagation.

2. THE STRUCTURE OF A ONE-HOP SIGNAL

A chirp ionosonde emits the continuous frequency-modulated signal

$$V(t) = a_0(t) \exp\left[-i\left(\omega_a t + \dot{\omega} t^2/2\right)\right] , \tag{1}$$

where ω_a is the initial frequency of the signal, $\dot{\omega}$ is its frequency-deviation rate, and $a_0(t)$ is a quantity equal to unity in the entire existence interval of the signal $V(t)$ and to zero outside that interval.

After the signal passes the ionospheric channel, we have, at the receiver output,

[1] Research Institute of Applied Physics, Irkutsk State University, Irkutsk, Russia; [2] Institute of Solar-Terrestrial Physics, Siberian Branch of the Russian Academy of Sciences, Irkutsk, Russia. Translated from Izvestiya Vysshikh Uchebnykh Zavedenii, Radiofizika, Vol. 43, No. 11, pp. 942–953, November, 2000. Original article submitted October 10, 2000.

$$U(t) = \int\limits_{-\infty}^{+\infty} U_{\rm s}(\omega, t) \exp(-i\omega t)\, {\rm d}\omega = \int\limits_{-\infty}^{+\infty} R(\omega, t) V_{\rm s}(\omega) \exp(-i\omega t)\, {\rm d}\omega, \tag{2}$$

where $U_{\rm s}(\omega, t)$ is the received-signal spectrum, $V_{\rm s}(\omega)$ is the emitted-signal spectrum, and $R(\omega, t)$ is the reflection coefficient of the quasistationary ionosphere.

Taking into account the signal-processing technique in a chirp ionosonde, it is easy to show that the output signal of the ionosonde is determined by the following expression [7–9, 12]:

$$S(\Omega) = \frac{1}{2\pi} \int\limits_{-\infty}^{+\infty} V(t) U^*(t) W(t) \exp(i\Omega t)\, {\rm d}t = \frac{1}{2\pi} \iint\limits_{-\infty}^{+\infty} V_s^*(\omega) R^*(\omega, t) V(t) W(t) \exp[it\,(\omega + \Omega)]\, {\rm d}t\, {\rm d}\omega, \tag{3}$$

where $W(t)$ is the weighting function describing the spectrum-analyzer time window. For simplicity, it is further approximated by the expression

$$W(t) = \exp\left[-(t - t_0)^2 / 2T^2\right],$$

where T is the time-window duration. Squaring Eq. (3) and averaging the result over the ensemble of realizations of a randomly inhomogeneous medium, we can obtain the following formula for the mean power spectrum $\langle |S(\Omega)|^2 \rangle$:

$$\begin{aligned} \left\langle |S(\Omega)|^2 \right\rangle = \frac{1}{(2\pi)^2} \iiint\limits_{-\infty}^{+\infty} V_s^*(\omega_1) V_s^*(\omega_2) W^*(t_1) W^*(t_2) V^*(t_1) V(t_2) \\ \times \exp[-it_1\,(\omega_1 + \Omega) + it_2\,(\omega_2 + \Omega)]\, \Gamma(\omega_1, \omega_2, t_1, t_2)\, {\rm d}t_1\, {\rm d}t_2\, {\rm d}\omega_1\, {\rm d}\omega_2, \end{aligned} \tag{4}$$

where $\Gamma(\omega_1, \omega_2, t_1, t_2) = \langle R^*(\omega_1, t_1) R(\omega_2, t_2) \rangle$ is the frequency-coherence function of the wave-field fluctuations in the quasistationary ionosphere.

In practice, T is of the order of 1 s and the frequency-deviation rate is 50–100 kHz/s. Therefore, we can assume that signal (1) is narrow-band in the interval T and that its spectrum is defined as

$$V_{\rm s}(\omega) = \frac{1}{\sqrt{2\pi\dot\omega}} \exp\left[\frac{i\,(\omega - \omega_a)^2}{2\dot\omega} - i\frac{\pi\, {\rm sgn}(\dot\omega)}{4}\right] \begin{cases} 1, & \omega_a < \omega < \omega_b; \\ 0, & \omega < \omega_a, \quad \omega > \omega_b, \end{cases} \tag{5}$$

where $\omega_b = \omega_a + \dot\omega T$. Introducing the summation and difference variables

$$\omega_{1,2} = \omega \pm \Delta\omega/2, \quad t_{1,2} = t \pm \Delta t/2$$

and allowing for the weak dependence of Γ on t_1 and t_2, we make calculations in Eq. (4) to yield

$$\left\langle |S(\Omega)|^2 \right\rangle = \frac{T\sqrt{\pi}}{(2\pi)^2\, \dot\omega} \int\limits_{-\infty}^{+\infty} \varphi_{\rm r}(\omega_0 - \omega - \Omega, (\omega - \omega_0)/\dot\omega, \omega)\, {\rm d}\omega, \tag{6}$$

where $\omega_0 = (\omega_a + \omega_b)/2$ and

$$\begin{aligned} \varphi_{\rm r} = \frac{1}{\pi} \iint\limits_{-\infty}^{+\infty} \Gamma(\omega, \Delta\omega, \Delta t) \exp\left[-\frac{(\Delta t)^2\, \dot\omega^2 T^2}{4} \left(1 + \frac{1}{\dot\omega^2 T^4}\right) - \frac{T^2\, (\Delta\omega)^2}{4} + \frac{T^2\, \dot\omega\, \Delta t\, \Delta\omega}{2}\right] \\ \times \exp\left[i\, \Delta t\, (\omega_0 - \omega - \Omega) + \frac{i\, \Delta\omega\, (\omega - \omega_0)}{\dot\omega}\right] {\rm d}(\Delta\omega)\, {\rm d}(\Delta t). \end{aligned} \tag{7}$$

For the frequency-coherence function of the field, we take the expression obtained using the geometrical-optics approximation [13]:

$$\Gamma(\Delta\omega, \Delta t) \approx |A|^2 \exp\left[i\left(\Delta\omega\,\tau + \Delta t\,\omega_{\rm g}\right) - (\Delta\omega)^2\,\sigma_\tau^2/2\right], \tag{8}$$

where $\tau(\omega_0)$ and $\omega_{\rm g}$ are, respectively, the propagation time and the Doppler frequency shift of the geometric-optical wave in the nonstationary ionosphere, A is the wave amplitude, and σ_τ^2 is the variance of the propagation time.

Note that the method of smooth perturbations was used in [14, 15] to describe the frequency-coherence function of the field with allowance for diffraction phenomena. In our paper, Eq. (8) is obtained under the condition of a strong dispersion of the wave phase, when diffraction phenomena contribute insignificantly to the field fluctuations and the main characteristics of the field are determined by effects arising from large-scale irregularities with characteristic dimensions $l \gg R_{\rm F}$ ($R_{\rm F}$ is the radius of the first Fresnel zone) [16].

Substituting Eq. (8) into Eq. (7) and performing the integration in Eq. (6), we get

$$\left\langle |S(\Omega)|^2 \right\rangle = \frac{|A|^2\,T}{2\pi F} \exp\left[-\frac{(\Omega - \omega_{\rm g} - \tau\dot\omega)^2}{F^2}\right], \tag{9}$$

where

$$F = \sqrt{T^{-2} + 2\dot\omega^2\sigma_\tau^2 + (\tau'\dot\omega^2 T)^2}$$

is the line width observed by the spectrum analyzer at the frequency $\Omega = \tau(\omega_0)\dot\omega + \omega_{\rm g}$ and $\tau' = \partial\tau(\omega_0)/\partial\omega_0$.

As seen from Eq. (9), the chirp-ionosonde resolution is determined by three factors: the frequency band $1/T$ of the spectrum-analyzer window, the variance σ_τ^2 of the random propagation time, and the dispersion distortions in the ionosphere (the third term of the radicand in the expression for the function F). It is easily seen that the contribution of the first term can be decreased by increasing the analysis-time T. In this case, however, the contribution of the second term remains the same, whereas the contribution of the dispersion distortions increases. Usually, however, the role of the dispersion distortions is insignificant, since τ' is small.

Using Eq.(9), we performed a numerical simulation of the spectrum $\langle |S(\Omega)|^2 \rangle$ of a chirp signal for one-hop propagation along a path of length $D = 3000$ km. The statistical moments of the propagation path were calculated using the method presented in [17]. As a model of the regular ionosphere, we chose the exponential dependence of the dielectric permittivity on the height:

$$\varepsilon = 1 - \frac{f_{\rm k}^2}{f^2} \exp\left[-\left(\frac{z - z_{\rm m}}{y_{\rm m}}\right)^2\right]. \tag{10}$$

For our calculations, we chose parameters typical of the F_2 layer: $z_{\rm m} = 270$ km, $y_{\rm m} = 80$ km, and $f_{\rm k} = 7$ MHz. Figure 1 shows the results of calculations of the chirp-signal spectrum (hereafter, the window duration of the spectrum analyzer is $T = 1$ s) for one-hop propagation with allowance for the dispersion distortions (Fig. 1a) as well as for the distortions due to both the medium dispersion and the influence of random ionospheric irregularities (Fig. 1b). Calculations were performed for the frequency $f = 16$ MHz (the ratio of the operating frequency and the maximum usable frequency $f_{\rm MUF}$ was equal to 0.6) at the frequency-deviation rate of the chirp signal 100 kHz/s. Inhomogeneity of electron density was characterized by the Gaussian dielectric-permittivity correlation function $\psi_\varepsilon(\mathbf{r}_1, \mathbf{r}_2) = \nu \exp\left[-(\mathbf{r}_1 - \mathbf{r}_2)^2/l^2\right]$ describing the mutual dependence of the electron-density fluctuations at the points with coordinates $\mathbf{r}_1$ and $\mathbf{r}_2$, where ν and l are , respectively, the intensity and scale of irregularities. As expected (see Eq. (9)), radio-wave scattering results in additional (with respect to the influence of the ionospheric dispersion [8, 9]) broadening of the signal spectrum. Here the irregularity parameters were chosen as follows: $\nu = 10^{-6}$ and $l = 1$ km. Analysis of calculations of spectra $\langle |S(\Omega)|^2 \rangle$ for other ratios $f/f_{\rm MUF}$ showed that the distortions of the chirp-signal spectrum are determined mainly by the behavior of the frequency-coherence radii of the fields of both propagation modes.

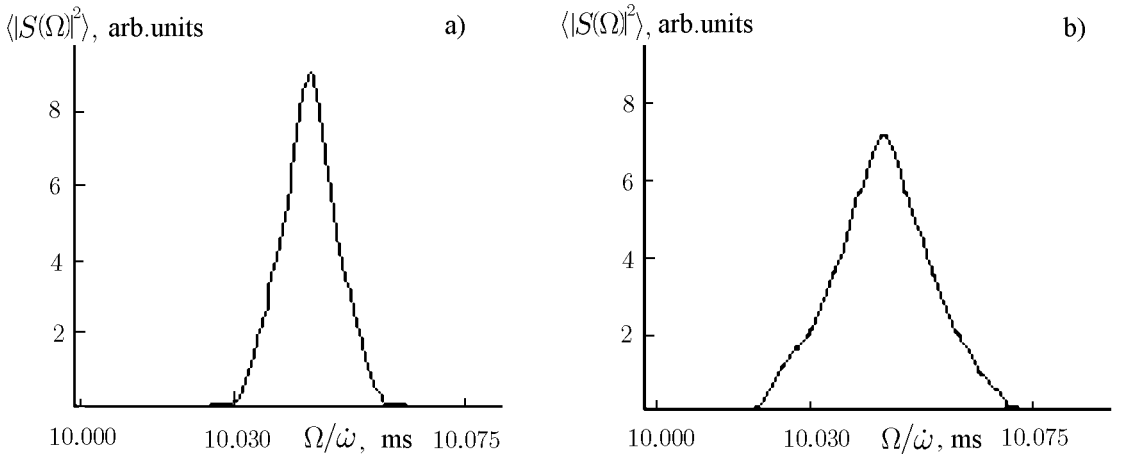

Fig. 1. Results of numerical simulation of the chirp-signal spectrum for the case of one-hop propagation with allowance (a) for only the dispersion distortions and (b) for the distortions due to both the medium dispersion and the influence of random ionospheric irregularities.

The radii, in turn, decrease as the sounding frequency tends to the maximum usable frequency under the condition of a strong phase dispersion (high-intensity irregularities) [18]. Thus it follows from the theoretical calculations that the spectrum of the chirp signal for both modes tends to increase as the operating frequency approaches the maximum usable frequency.

3. THE STRUCTURE OF A TWO-HOP SIGNAL

For two-hop propagation, the signal power spectrum at the chirp-ionosonde output can be determined using Eq. (9) as well. In this case, we will assume that the waves undergo specular reflection from the ground and that the fluctuations of the path characteristics are the sums of the fluctuations of these characteristics at each hop.

Figure 2 presents the envelopes of the chirp-signal spectra for two-hop propagation along the chosen path with the same parameters of irregularities as for Fig. 1. Here, the influence of random irregularities (see Fig. 2b) on the signal-structure distortions is also particularly pronounced. In this case, the signal-spectrum width is larger than that for one-hop propagation. This is related to the increase in the length of the scattering region in the ionosphere for two-hop propagation. At the same time, a significant (greater than 100 μs) broadening of the chirp-signal spectrum for two-hop propagation, observed in oblique-sounding experimental ionograms in some cases [19], does not appear here. Such a discrepancy between the theoretical calculations and the measurement data requires the analysis of other factors leading to such significant distortions of the chirp signal.

First of all, the signal structure on a two-hop path was simulated under the assumption of the specular reflection of waves from the boundary of the Earth–ionosphere waveguide, which seems inadequate. Allowing for the actual profile of the ground, one should take into account the possibility of the additional scattering of ionospheric radio waves [18, 20] and, hence, one can expect changes in the correlation properties of the short-wave field. Therefore, for a more accurate description of the chirp signal in the case of two-hop propagation, one needs, strictly speaking, the knowledge of the frequency-coherence function $\Gamma(\omega_1, \omega_2, t_1, t_2)$ of the field with allowance for scattering by the Earth's rough surface.

Usually [16, 21], when solving the problem on wave scattering by a rough surface, the incidence of a regular plane or spherical wave on this surface is considered. The problem of scattering of short radio waves, reflected from the ionosphere, by the ground is more complicated, since the structure of the incident ionospheric radio wave comprises distortions due to regular refraction and wave scattering in the inhomogeneous ionosphere. Allowing for the fact that, for multiple-hop propagation of short radio waves, the forward scattering by ground roughnesses is the most significant, we will mainly take the large-scale

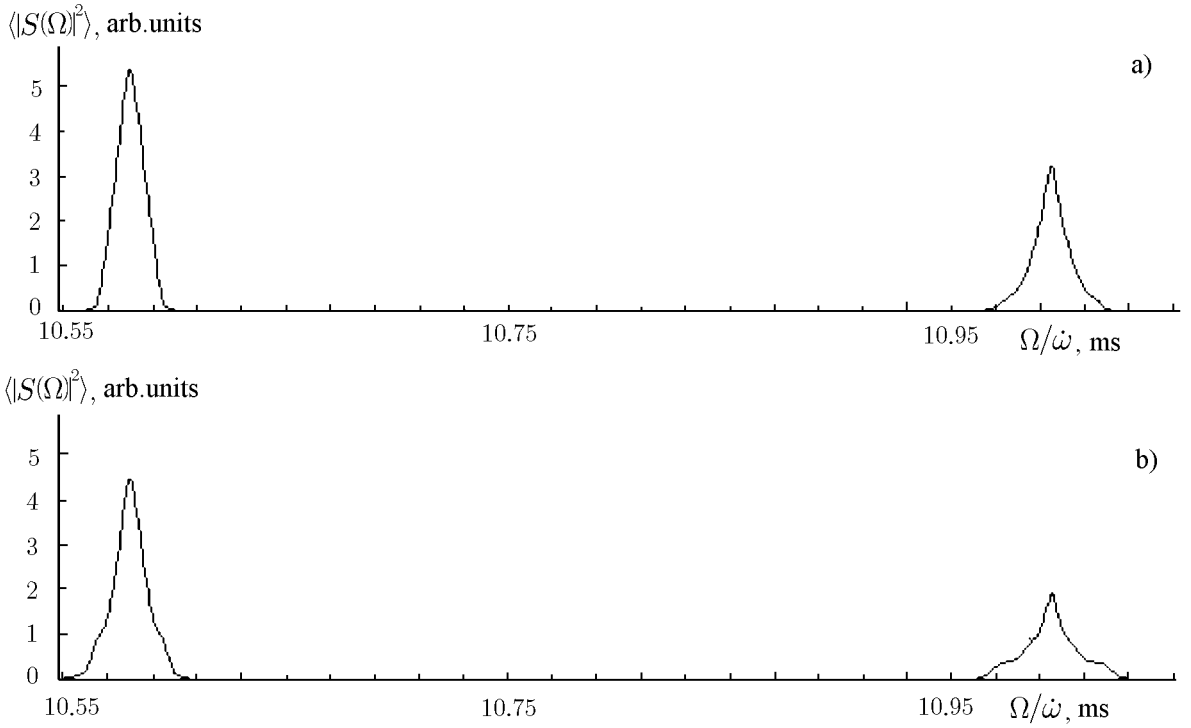

Fig. 2. Results of numerical simulation of the spectra of the upper and lower rays of a chirp signal for two-hop propagation with allowance (a) for only the dispersion distortions and (b) for the distortions due to both the medium dispersion and the influence of random ionospheric irregularities.

roughnesses into account. Within the framework of this assumption, scattering of ionospheric radio waves by the ground can be calculated using the Kirchhoff method [16].

Within the framework of the Kirchhoff method, one can obtain the following expression for the wave field scattered by the Earth:

$$U = \int V_{\rm E}(\mathbf{r}')\frac{\partial}{\partial N}[U_0(\mathbf{r}')G(\mathbf{r}',\mathbf{r})]\,{\rm d}L, \tag{11}$$

where $U_0(\mathbf{r}')$ is incident-wave field, $G(\mathbf{r}',\mathbf{r})$ is the Green's function, $\mathbf{N}$ is the normal to the rough surface L, and $V_{\rm E}(\mathbf{r}')$ is the coefficient of reflection from the Earth.

We will use the geometric-optical approximation for the incident-wave field and the Green's function and, for simplicity, consider the problem of scattering by the Earth's surface in a two-dimensional case (neglecting the scattering in the azimuthal plane). Now the coordinate x corresponds to the distance along an unperturbed (smooth) Earth's surface, and the coordinate z, to the height measured from this surface. In this case,

$$U = -\int V_{\rm E} q_z A_0(x') A_{\rm G}(x',x)\exp[i\Phi_0(x') + i\Phi_{\rm G}(x',x) - iq_z\xi(x')]\,{\rm d}x', \tag{12}$$

where A_0 and Φ_0 are, respectively, the amplitude and phase of the incident wave, $A_{\rm G}$ and $\Phi_{\rm G}$ are, respectively, the amplitude and phase of the Green's function, q is the wave vector of the scattered radiation at the ground, and $\xi(x')$ is the function characterizing the ground roughness.

Assuming that ionospheric irregularities affect mainly the phase of the wave rather than its amplitude (this is quite permissible in the framework of the ray approximation), we can neglect the amplitude fluctuations. Then, using Eq. (12), we can obtain an expression for the frequency-coherence function $\Gamma(\omega_1,\omega_2,t_1,t_2)$ of the field. Assuming that the ray path in the ionosphere crosses a large number of irregularities, i.e., the Gaussian distribution law holds for the phase fluctuations, we have

$$\Gamma(\omega_1,\omega_2,t_1,t_2)=\iint V_{\rm E}^2 q_z^2\,|A_1(x_1)A_2(x_1,x)|^2\exp\Big[i\Phi_1(x_1,\omega_1 t_1)+i\Phi_2(x_1,\omega_1 t_1,x)$$
$$-i\Phi_1(x_2,\omega_2 t_2)-i\Phi_2(x_2,\omega_2 t_2)-\frac{i}{2}\Big\langle[\tilde\Phi_1(x_1,\omega_1 t_1)+\tilde\Phi_2(x_1,\omega_1 t_1)-\tilde\Phi_1(x_2,\omega_2 t_2) \tag{13}$$
$$-\tilde\Phi_2(x_2,\omega_2 t_2)-q_z(\omega_1)\xi(x_1)+q_z(\omega_2)\xi(x_2)]^2\Big\rangle\Big]\,{\rm d}x_1\,{\rm d}x_2,$$

where A_1 and A_2 are the field amplitudes at the first and second hops, respectively, and Φ_1 and Φ_2 are the field phases at the first and second hops, respectively. Introducing the summation and difference variables $x_1-x_2=\xi$ and $x_1+x_2=2\eta$ and setting $\omega_2=\omega_1+\Delta\omega$ and $t_2=t_1+\Delta t$, we perform the integration and obtain

$$\Gamma(\omega_1,\omega_2,t_1,t_2)\approx\sqrt{2\pi}\int\sigma_{\rm p}^{-1}V_{\rm E}^2q_z^2\,|A_1(\eta)A_2(\eta)|^2\exp\!\left(-\frac{q_x^2}{2\sigma_{\rm p}^2}\right)M(\eta)\,{\rm d}\eta, \tag{14}$$

where

$$M=\exp[-i\tau'\,\Delta\omega-i\omega_{\rm g}\,\Delta t-(\sigma'_\tau\,\Delta\omega)^2/2],$$
$$q_z=-k\left(\sqrt{1-S_1^2}+\sqrt{1-S_2^2}\right),\quad q_x=-k\,(S_1-S_2),\quad \tau'=\tau+\frac{q_x\psi_{x\tau}}{\sigma_{\rm p}^2}\,,$$

$S_1=\sin\beta_{r1}$, $S_2=\sin\beta_{r2}$, k is the wave number, β_{r1} and β_{r2} are, respectively, the incidence and reflection angles at the scattering point on the ground,

$$\sigma_\tau'^2=\sigma_\tau^2-\frac{\psi_{x\tau}^2}{\sigma_{\rm p}^2}\,,\quad \sigma_\tau^2=\sigma_{\tau1}^2+\sigma_{\tau2}^2+\left(\frac{\partial q_z}{\partial\omega}\right)^2\sigma_{\rm E}^2,$$

$$\sigma_{\rm p}^2=\sigma_{\beta1}^2+\sigma_{\beta2}^2+q_z^2\sigma_r^2,\quad \psi_{x\tau}=\psi_{x\tau1}+\psi_{x\tau2},$$

$\sigma_{\tau1}^2$ and $\sigma_{\tau2}^2$ are the variances of the ray propagation time at the first and second hops, respectively, $\sigma_{\beta1}^2$ and $\sigma_{\beta2}^2$ are the variances of the ray-arrival angles at the first and second hops, respectively, $\psi_{x\tau1}$ and $\psi_{x\tau2}$ are the mutual-correlation functions of fluctuations of the distance and propagation time, respectively, of rays at the hops, $\sigma_{\rm E}^2=\langle\xi^2\rangle$ is the variance of the roughness amplitude of the Earth's surface, and $\sigma_r^2=\Big\langle(\partial\xi/\partial\eta)^2\Big\rangle$.

Substituting Eq. (14) into Eq. (7) and performing the integration in Eq. (6), we obtain the following expression for the chirp-signal spectrum on the two-hop path:

$$|S(\Omega)|^2=\frac{T}{\sqrt{2\pi}}\int(\sigma_{\rm p}\Theta)^{-1}V_{\rm E}^2q_z^2\,|A_1(\eta)A_2(\eta)|^2\exp\!\left[-\frac{q_x^2}{2\sigma_{\rm p}^2}-\frac{(\Omega-\omega_{\rm g}-\tau'\dot\omega)^2}{\Theta^2}\right]\,{\rm d}\eta, \tag{15}$$

where $\Theta=\sqrt{T^{-2}+2\dot\omega^2\sigma_\tau'^2+(\tau'\dot\omega^2T)^2}$.

Equation (15) was used to simulate numerically the signal-spectrum distortions for various parameters of ionospheric irregularities and ground roughnesses. The roughness of the Earth's surface was described by the Gaussian correlation function with the parameters μ and p, where $\sqrt{\mu}$ is the standard deviation of the height and p is the spatial-correlation radius of ground roughnesses. As an example, Fig. 3 shows the results of calculations of the mean power spectrum $\langle S(\Omega)|^2\rangle$, where the parameters of ionospheric irregularities were chosen as above ($\nu=10^{-6}$ and $l=1$ km), $\mu=10^{-2}$, and the scale p took the values 10.5 and 3 km. It is easy to see that, due to scattering from the ground roughness, a wide temporal plateau appears in the chirp-signal spectrum, which disappears upon smoothing the roughness. The feature of the plateau dynamics in the chirp-signal spectrum is that it transforms to additional modes with an increase in the scale of the ground roughness (see Figs. 3b and 3c). The trace analysis showed that such modes correspond to combined ways of radio wave propagation. After reflection from the ionosphere, the bundle of lower rays

of the first hop, scattering by the roughnesses of the Earth's surface, further propagates in the upper way, i.e., it transforms to the bundle of upper rays of the second hop (mode III in Fig. 3c). On the other hand, the bundle of upper rays of the first hop transforms to the bundle of lower rays of the second hop upon scattering by the Earth (mode IV in Fig. 3c). Since the energies transferred by the lower and upper rays are different due to a large divergence of the upper rays, the energy contribution of mode III is more pronounced in the chirp-signal spectrum and, in the sense of a temporal delay, this mode is adjacent to the fundamental mode I corresponding to the two-hop lower-ray propagation. Combined mode IV has a temporal delay close to that of the fundamental mode II corresponding to the two-hop upper-ray propagation. We note that due to multiple wave scattering by the ionosphere and the roughnesses of the Earth's surface, one should expect, for multiple-hop paths, an increase in the number of additional combined modes not relating directly to the regular structure of the ionosphere. This circumstance should apparently be taken into account when solving the problem of forecasting the mode composition of the long-range radiocommunication signals.

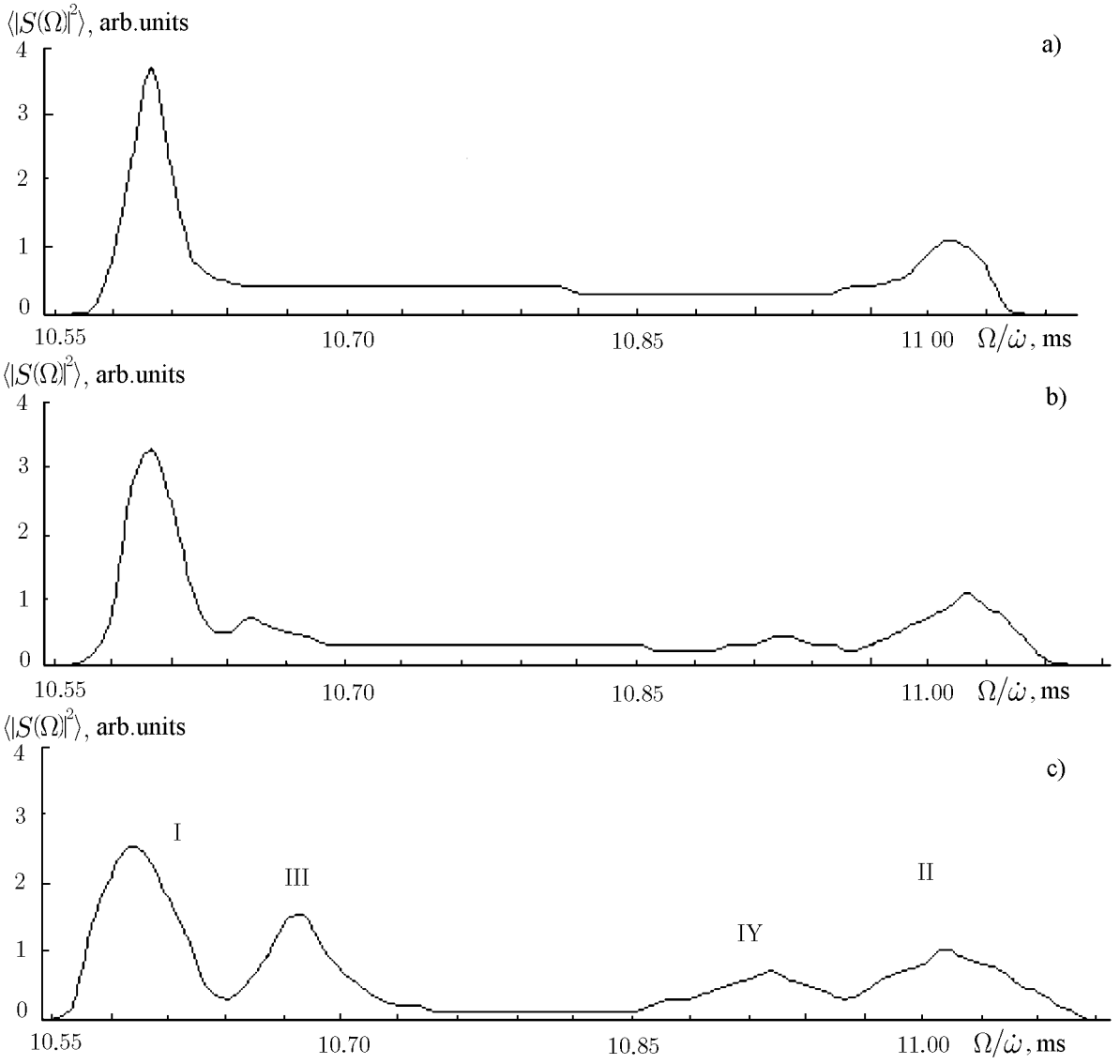

Fig. 3. Results of numerical simulation of the chirp-signal spectrum in the case of two-hop propagation with allowance for the distortions due to both the medium dispersion and the influence of random ionospheric irregularities and ground roughnesses, for the spatial-correlation radii of ground roughnesses (a) $p = 3$ km, (b) $p = 5$ km, and (c) $p = 10$ km.

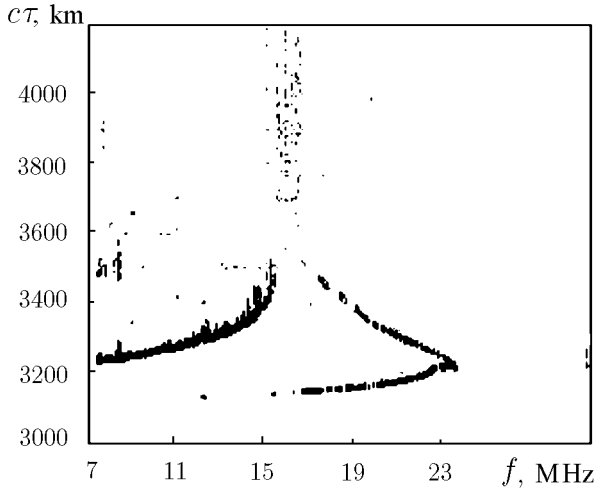

Fig. 4. Typical ionogram of oblique sounding under the quiet ionospheric conditions for the Irkutsk–Magadan path (11:41:00 UT, February 15, 1989).

To make a comparison with the above results of theoretical calculations, we analyzed the experimental chirp-ionosonde data for the Magadan–Irkutsk path. The path length was $D = 3000$ km. The technical characteristics of the used devices were given in [4], the frequency-deviation rate was 100 kHz/s, and the sampling duration (time-window duration) was $T = 1$ s. For processing, we chose sessions with a typical structure of ionograms (see Fig. 4). We have chosen 100 ionograms recorded in May and October, 1989; February, 1994; and February, 1995. The processing was made in three stages.

At the first stage, we made a preliminary processing and identification of the propagation modes [22]. At the second stage, using the interactive regime, we determined the maximum usable frequencies f_{MUF} of the corresponding modes of a received signal. At the third stage, we determined an equivalent duration τ_{eq} of the power spectrum in the frequency band $(0.85–1.00)f/f_{\mathrm{MUF}}$ with frequency spacing 94 kHz ($\tau_{\mathrm{eq}} = \delta\Omega/\dot{\omega}$, where $\delta\Omega$ is the width of the power-spectrum envelope at the level 0.5 or 0.1). We note that in the absence of any distortion in the ionospheric channel, $\tau_{\mathrm{eq}} = 30$ μs for the chosen processing parameters. We determined τ_{eq} in the automatic regime for the one-hop signal and in the interactive regime for the two-hop signal.

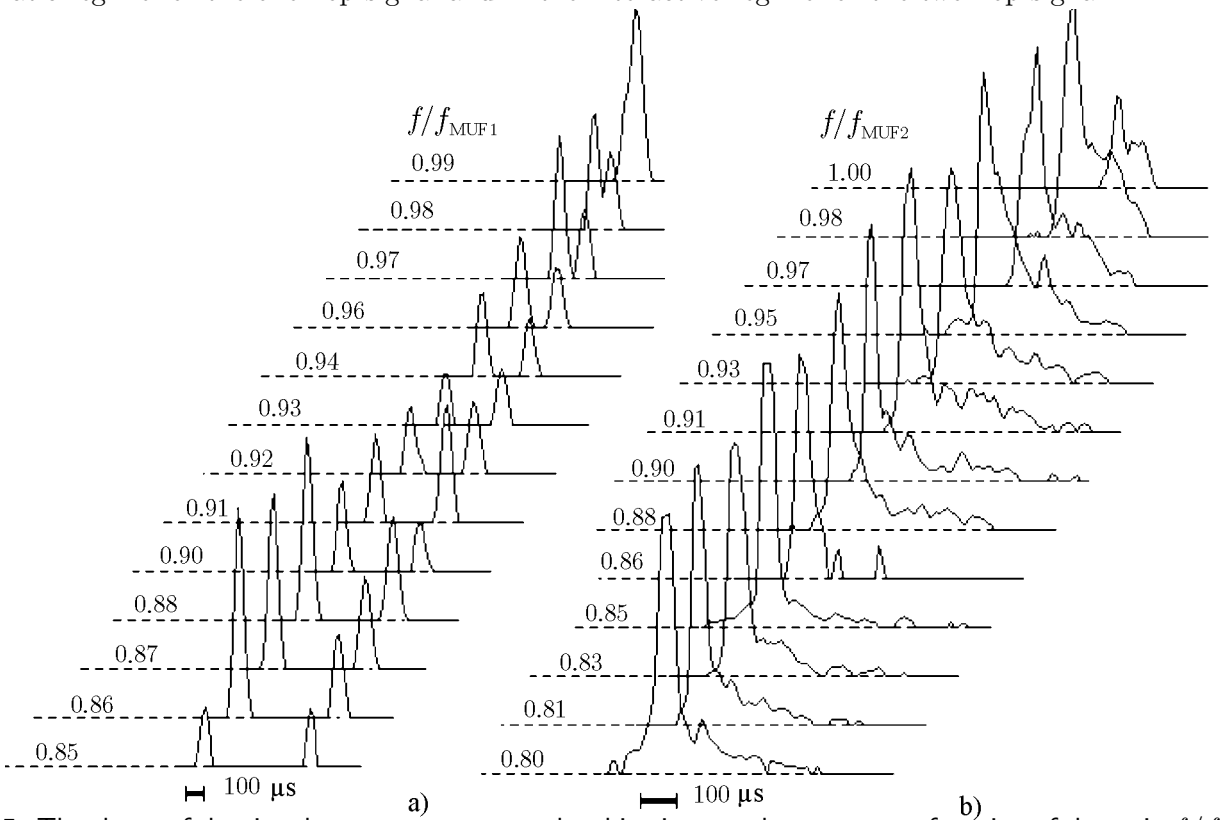

Fig. 5. The shape of the signal power spectrum at the chirp-ionosonde output as a function of the ratio f/f_{MUF} for the case shown in Fig. 4: (a) the shape of the power spectrum of a one-hop signal (on the left and right are the power spectra of the lower and upper modes, respectively) and (b) the shape of the power spectrum of a two-hop signal.

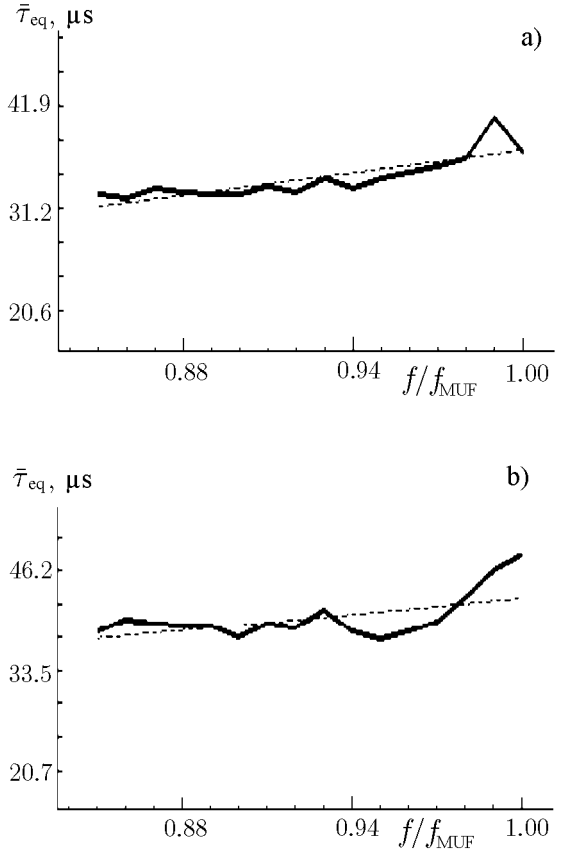

Fig. 6. Experimental dependence of the mean equivalent duration $\bar{\tau}_{\rm eq}$ of the power spectrum of a one-hop signal at the level 0.5 on the ratio $f/f_{\rm MUF}$: (a) $\bar{\tau}_{\rm eq}$ for the lower mode and (b) $\bar{\tau}_{\rm eq}$ for the upper mode. The dotted line shows the linear approximation of the experimental dependence.

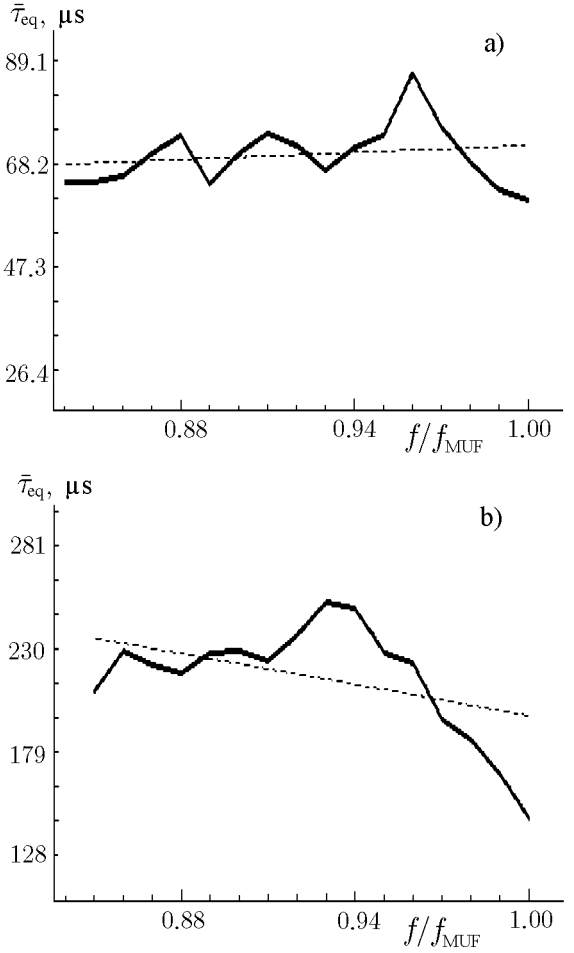

Fig. 7. Experimental dependence of the mean equivalent duration of the power spectrum of a two-hop signal on the ratio $f/f_{\rm MUF}$: (a) the duration $\bar{\tau}_{\rm eq}$ determined at the level 0.5 and (b) the duration $\bar{\tau}_{\rm eq}$ determined at the level 0.1. The dotted line shows the linear approximation of the experimental dependence.

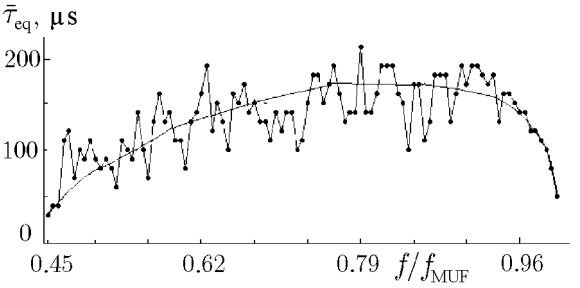

Fig. 8. Experimental dependence of the mean equivalent duration $\bar{\tau}_{\rm eq}$ of the power spectrum of a two-hop signal on the ratio $f/f_{\rm MUF}$ in a wide frequency band (05:03 UT, February 15, 1995).

Figure 5 shows typical power spectra for the one- and two-hop signals (Figs. 5a and 5b, respectively). The presence of a plateau (significant increase in the $\tau_{\rm eq}$ determined at the level 0.1) is typical of the case of a two-hop signal, which is in agreement with the above-presented numerical results (see Fig. 3). Upon determining a few values of $\tau_{{\rm eq},i}$ for each ratio $f/f_{\rm MUF}$, we calculate the mean value $\tau_{\rm eq} = n^{-1}\sum_i \tau_{{\rm eq},i}$, where n is the number of values of $\tau_{\rm eq}$ obtained for the same ratio $f/f_{\rm MUF}$ ($n_{\max} = 100$ is determined by the number of chosen ionograms). The results of processing are given in Figs. 6 and 7.

Analysis of the data obtained shows that, for the lower $1F$ mode (see Fig. 6a), the mean value of τ_{eq} varies from 32 to 39 μs as the operating frequency increases. For the upper $1F$ mode (see Fig. 6b), $\bar{\tau}_{\text{eq}}$ varies from 38 to 50 μs with increasing operating frequency. The characteristic behavior of $\bar{\tau}_{\text{eq}}$ for both modes corresponds to the variation of the frequency-coherence function with the frequency [13].

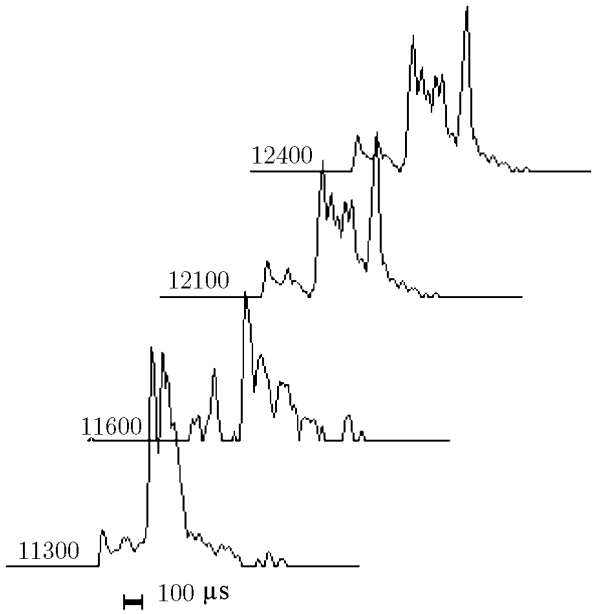

Fig. 9. Example of the appearance of additional multipath propagation in a narrow frequency band. On the left is the frequency f in kHz.

For a two-hop signal (see Fig. 7), a more significant increase in $\bar{\tau}_{\text{eq}}$ is observed and the value of $\bar{\tau}_{\text{eq}}$ determined at the level 0.5 varies from 65 to 88 μs with increasing frequency. Its increase rate is somewhat greater than that for a one-hop signal. In the band $(0.98–1)f/f_{\text{MUF}}$, $\bar{\tau}_{\text{eq}}$ decreases.

Variation in the value of the quantity $\bar{\tau}_{\text{eq}}$ determined at the level 0.1 exhibits more complicated behavior. This quantity varies from 213 to 150 μs in the band $(0.85–1)f/f_{\text{MUF}}$ with increasing frequency (see. Fig. 7b). If we consider the character of variation of $\bar{\tau}_{\text{eq}}$ in a wider band, the plateau tends to increase with the frequency. Then, starting from a certain frequency, a decrease in $\bar{\tau}_{\text{eq}}$ is observed as the frequency approaches f_{MUF} (see Fig. 8).

In separate sessions for a two-hop signal, the effect of additional multipath propagation appears to occur in a narrow frequency band. An example of such a case is shown in Fig. 9. This effect, pointed out in our numerical simulation (see. Fig. 3), is possible in the case of a path over the territory with a mountain accident, which is typical of the Irkutsk–Magadan path.

5. CONCLUSIONS

The presented results of our numerical simulation and the experimental data show that the proposed method for calculating the structure of output signals of chirp ionosondes provides a correct qualitative presentation of a number of effects caused by the influence of the ionospheric irregularities and the ground roughness which give the main contribution to the change in the signal structure. For two-hop signals, the ground roughness plays a dominant role. The influence of the ionospheric irregularities and the ground roughness decreases considerably the resolution of chirp ionosondes and must be taken into account when calculating the pass properties of the ionospheric communication channel.

We thank the editor for his extensive work on improving the quality of the paper. The present work was supported by the Russian Foundation for Basic Research (project Nos. 98–02–16023 and 00–02–17780).

REFERENCES

1. G. H. Barry and R. B. Fenwick, in: T. B. Jones, ed., *AG ARD Conference Proceedings*, No. 13, 487 (1969).
2. V. A. Ivanov, V. A. Frolov, and V. V. Shumaev, *Izv. Vyssh. Uchebn. Zaved., Radiofiz.*, **29**, No. 2, 235 (1986).
3. G. F. Earl and B. D. Ward, *Radio Sci*, **22**, No. 2, 275 (1987).
4. I. G. Brynko, I. A. Galkin, V. P. Grozov, et al., *Adv. Space Res.*, **8**, No. 4, 121 (1988).
5. L. C. A. Paul and S. C. Paul, *Annali di Geofisica*, **36**, No. 2, 135 (1994).

6. Lynn, in: *INAG-62*, Sangary (1998), p. 14.
7. N. V. Ilyin, V. V. Khakhinov, V. I. Kurkin, et al., in: *Proceedings of ISAP'96, Vol. 3*, Chiba, Japan, 689 (1996).
8. B. Lunborg and M. Lungren, *J. Atmos. Terr. Phys.*, **54**, No. 3–4, 311 (1992).
9. N. D. Filipp, N. Sh. Blaunshtein, L. M. Erukhimov, et al., *Modern Methods for Studying Dynamic Processes in the Ionosphere* [in Russian], Shtiintsa, Kishinev (1991).
10. S. Solous, *Radio Sci.*, **24**, No. 4, 585 (1989).
11. B. G. Barabashov and G. G. Vetrogradov, *Izv. Vyssh. Uchebn. Zaved. Severokavkaz. Reg., Estestv. Nauki*, No. 3, 39 (1994).
12. B. N. Gershman, L. M. Erukhimov, and Yu. Ya. Yashin, *Wave Phenomena in the Ionosphere and Space Plasma* [in Russian], Nauka, Moscow (1984).
13. N. T. Afanas'yev, V. P. Grozov, A. A. Krasikov, et al., in: *Research on Geomagnetism, Aeronomy, and Solar Physics* [in Russian], No. 63, Nauka, Moscow (1983), p. 180.
14. V. E. Gherm, N. N. Zernov, and B. Lundborg, *J. Atmos. Solar-Terr. Phys.*, **59**, No. 14, 1843 (1997).
15. V. E. Gherm, N. N. Zernov, B. Lundborg, and A. Vustberg, *J. Atmos. Solar-Terr. Phys.*, **59**, No. 14, 1831 (1997).
16. S. M. Rytov, Yu. A. Kravtsov, and V. I. Tatarskii, *Introduction to Statistical Radiophysics, Vol. 2. Random Fields* [in Russian], Nauka, Moscow (1978).
17. N. T. Afanas'yev, V. P. Grozov, V. E. Nosov, and M. V. Tinin, in: *Research on Geomagnetism, Aeronomy, and Solar Physics* [in Russian], No. 84, Nauka, Moscow (1989), p. 77.
18. M. V. Tinin, N. T. Afanasiev, S. M. Mikheev, A. P. Pobedina, and O. V. Fridman, *Radio Sci.*, **27**, No. 2, 245 (1992).
19. I. I. Orlov, in: *Scientific Report on Project "Tazgun," Vol. 3* [in Russian], Irkutsk (1989).
20. N. T. Afanas'yev, A. P. Pobedina, and M. V. Tinin, in: *XIVth All-Union Conference on Radio Wave Propagation, Vol. 4* [in Russian], Kharkov (1990), p. 1.
21. F. G. Bass and I. M. Fuks, *Wave Scattering from Statistically Rough Surfaces*, Pergamon Press, New York (1979).
22. V. P. Grozov, V. I. Kurkin, V. I. Nosov, and S. N. Ponomarchuk, in: *Proceedings of ISAP'96*, Chiba, Japan (1996), p. 693.